Simulation of Soft-Switched Isolated DC-DC Converters for Auxiliary Railway Supply Using PWM Technique

P. Tulasi Ram
Department of Electronics and Electrical Engineering,
Avanthi institute of Engineering and Technology
Visakhapatnam, Andhra Pradesh - 535006, India.

V. Sarath Kumar
Department of Electronics and Electrical Engineering,
Avanthi institute of Engineering and Technology
Visakhapatnam, Andhra Pradesh - 535006, India.

Abstract:

In modern railways coaches, the electrical separation between the high voltage side and the auxiliary equipments on the consumer side is realized by means of heavy and bulky 50-Hz transformers. In order to reduce the weight and size of the devices, today new power supply systems are proposed that consist in soft-switched isolated dc-dc converters with a lightweight medium frequency transformer and diverse output modules supplied by a common 600 V dc intermediate circuit.

This paper aims to investigate in detail two such solutions of isolated dc-dc converters for auxiliary railway supply where zero-current transitions are achieved for the primary inverter switches. A comparison based on several criteria (overall power rating, losses in power semiconductor devices, operation in the whole range of load, etc.) is presented. Pulse width modulation is used to increase the fastness and to reduce the dc transients.

Keywords:

DC TO DC converter, PI controller, PWM

INTRODUCTION:

In Order to protect the natural environment on the earth, the development of clean energy without pollution has the major representative role in the last decade. By dealing with the issue of global warming, clean energies, such as fuel cell (FC), photovoltaic, and wind energy, etc., have been rapidly promoted [1].

Due to the electric characteristics of clean energy, the generated power is critically affected by the climate or has slow transient responses, and the output voltage is easily influenced by load variations. Besides, other auxiliary components, e.g., storage elements, control boards, etc., are usually required to ensure the proper operation of clean energy. For example, an FC-generation system is one of the most efficient and effective solutions to the environmental pollution problem. In addition to the FC stack itself, some other auxiliary components, such as the balance of plant (BOP) including an electronic control board, an air compressor, and a cooling fan, are required for the normal work of an FC generation system. In other words, the generated power of the FC stack also should satisfy the power demand for the BOP [2].

Thus, various voltage levels should be required in the power converter of an FC generation system. In general, various single-input single-output dc–dc converters with different voltage gains are combined to satisfy the requirement of various voltage levels, so that its system control is more complicated and the corresponding cost is more expensive. The motivation of this study is to design a single-input multiple-output (SIMO) converter for increasing the conversion efficiency and voltage gain, reducing the control complexity, and saving the manufacturing cost [3].
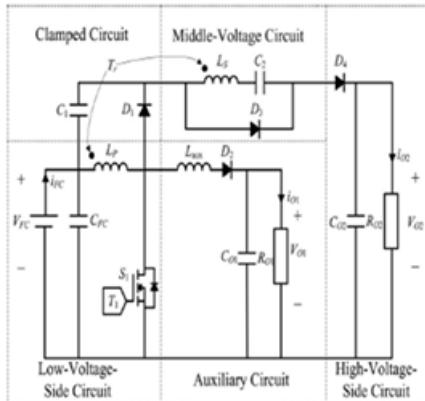
II. SIMO CONVERTER:

Fig 1. SIMO converter

In this paper presented a SIMO dc–dc converter capable of generating buck, boost, and inverted outputs simultaneously. However, over three switches for one output were required. This scheme is only suitable for the low output voltage and power application, and its power conversion is degenerated due to the operation of hard switching [4].

Proposed a new dc–dc multi-output boost converter, which can share its total output between different series of output voltages for low- and high-power applications Unfortunately, over two switches for one output were required, and its control scheme was complicated. Besides, the corresponding output power cannot supply for individual loads independently.

Investigated a multiple-output dc–dc converter with shared zero-current switching (ZCS) lagging leg. Although this converter with the soft-switching property can reduce the switching losses, this combination scheme with three full-bridge converters is more complicated, so that the objective of high-efficiency power conversion is difficult to achieve, and its cost is inevitably increased [5].
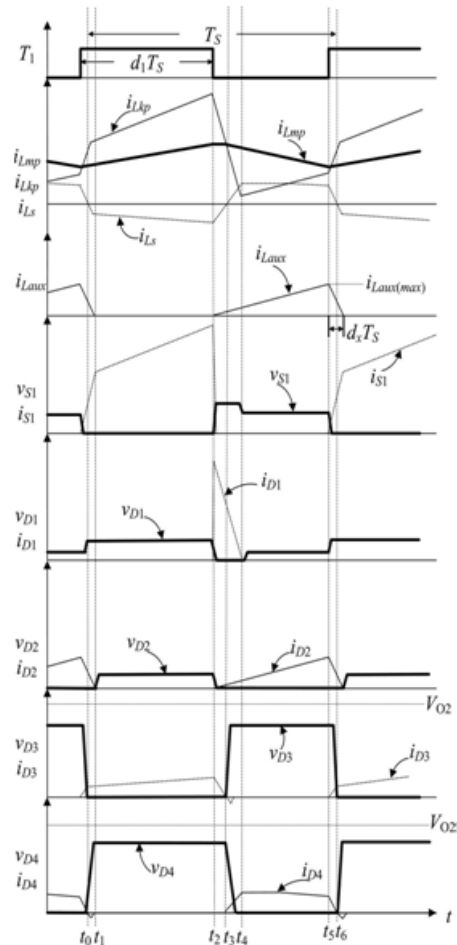

Fig 2 characteristics of proposed SIMO converter Operating Modes

Mode 1 (t0-t1)
Mode 2 (t1-t2)
Mode 3 (t2-t3)
Mode 4 (t3-t4)
Mode 5 (t4-t5)
Mode 6 (t5-t6)

Operating Modes Explanation
MODE 1 (t0-t1)

In this mode, the main switch S1 was turned ON for a span, and the diode D4 turned OFF. Because the polarity of the windings of the coupled inductor Tr is positive, the diode D3 turns ON [6]. The secondary current iLs reverses and charges to the middle voltage capacitor C2. When the auxiliary inductor Laux releases its stored energy completely, and the diode D2 turns OFF, this mode ends.
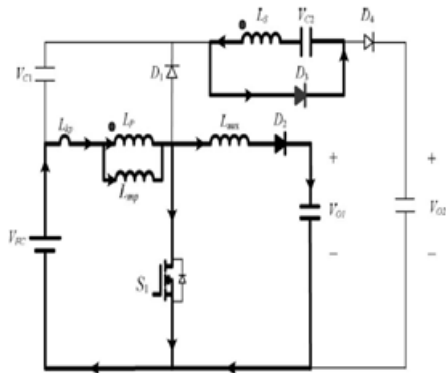
Fig2.1 operating mode (t0-t1)

MODE 2 (t1-t2)

At time t = t1, the main switch S1 is persistently turned ON. Because the primary inductor LP is charged by the input power source, the magnetizing current iLmp increases gradually in an approximately linear way. At the same time, the secondary voltage vLs charges the middle-voltage capacitorC2 through the diode D3. Although the voltage vLmp is equal to the input voltage VFC both at modes 1 and 2, the ascendant slope of the leakage current of the coupled inductor (diLkp /dt) at modes 1 and 2 is different due to the path of the auxiliary circuit [7]. Because the auxiliary inductor Laux releases its stored energy completely, and the diode D2 turns OFF at the end of mode 1, it results in the reduction of diLkp /dt at mode2.
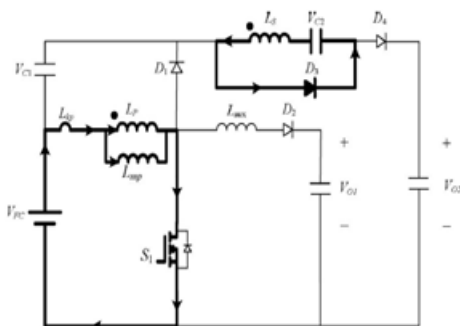

Fig2.2 operating mode (t1-t2)

MODE 3 (t2-t3)

At time t = t2 , the main switch S1 is turned OFF. When the leakage energy still released from the

secondary side of the coupled inductor, the diode D3 persistently conducts and releases the leakage energy to the middle-voltage capacitor C2. When the voltage across the main switch VS 1 is higher than the voltage across the clamped capacitor VC1, the diode D1 conducts to transmit the energy of the primary-side leakage inductor Lkp into the clamped capacitor C1. At the same time, partial energy of the primary-side leakage inductor Lkp is transmitted to the auxiliary inductor Laux, and the diode D2 conducts [8]. Thus, the current iL aux passes through the diode D2 to supply the power for the output load in the auxiliary circuit. When the secondary side of the coupled inductor releases its leakage energy completely, and the diode D3 turns OFF, this mode ends.
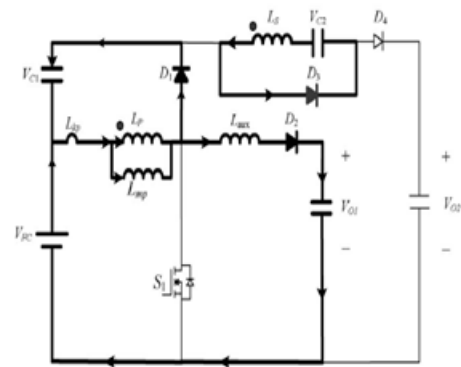

Fig2.3 operating mode (t2-t3)

MODE 4 (t3-t4)

At time t = t3, the main switch S1 is persistently turned OFF. When the leakage energy has released from the primary side of the coupled inductor, the secondary current iLS is induced in reverse from the energy of the magnetizing inductor Lmp through the ideal transformer, and flows through the diode D4 to the HVSC. At the same time, partial energy of the primaryside leakage inductor Lkp is still persistently transmitted to the auxiliary inductor Laux, and the diode D2 keeps conducting [9]. Moreover, the current iL aux passes through the diode D2 to supply the power for the output load in the auxiliary circuit.
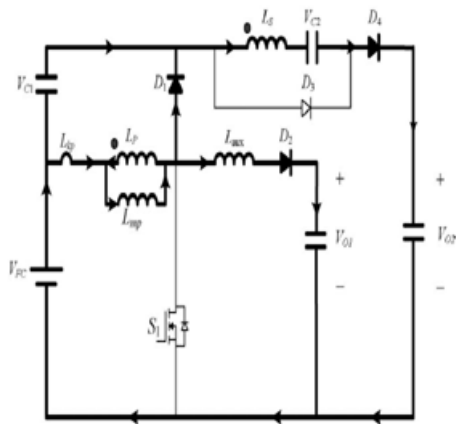
Fig2.4 operating mode (t3-t4)

MODE 5 (t4-t5)

At time t = t4, the main switch S1 is persistently turned OFF, and the clamped diode D1 turns OFF because the primary leakage current iLkp equals to the auxiliary inductor current iL aux. In this mode, the input power source, the primary winding of the coupled inductor Tr, and the auxiliary inductor Laux connect in series to supply the power for the output load in the auxiliary circuit through the diode D2. At the same time, the input power source, the secondary winding of the coupled inductor Tr , the clamped capacitor C1 , and the middle voltage capacitor (C2) connect in series to release the energy into the HVSC through the diode D4 [10] .

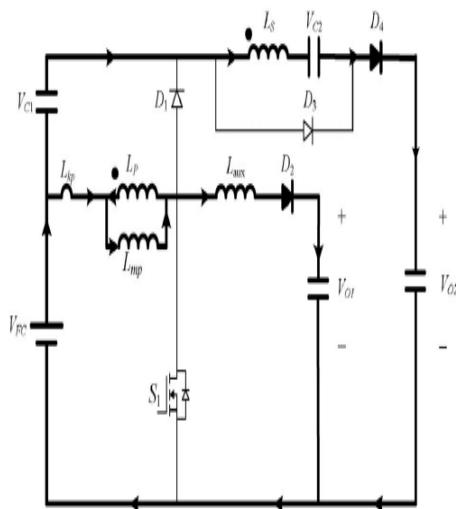Fig2.5 operating mode (t4-t5)

MODE 6 (t5-t6)

At time t=t5, this mode begins when the main switch S1 is triggered. The auxiliary inductor current iL aux needs time to decay to zero, the diode D2 persistently conducts. In this mode, the input power source, the clamped capacitor C1 , the secondary winding of the coupled inductor Tr , and the middle-voltage capacitor C2 still connect in series to release the energy into the HVSC through the diodeD4.Since the clamped diodeD1 can be selected as a low-voltage Schottky diode, it will be cut off promptly without a reverse-recovery current.Moreover, the rising rate of the primary current iLkp is limited by the primary-side leakage inductor Lkp. Thus, one cannot derive any currents from the paths of the HVSC, the middle-voltage circuit, the auxiliary circuit, and the clamped circuit. As a result, the main switch S1 is turned ON under the condition of ZCS and this soft-switching property is helpful for alleviating the switching loss. When the secondary current iLS decays to zero, this mode ends. After that, it begins the next switching cycle and repeats the operation in mode 1 [11].
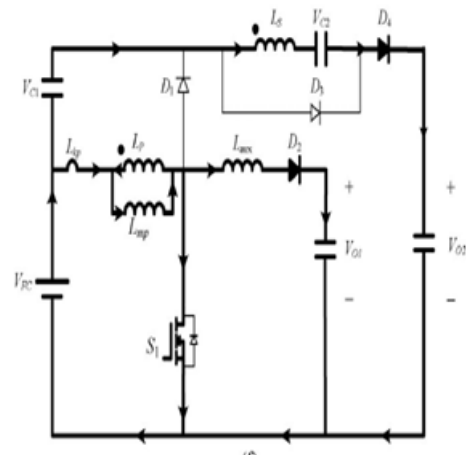

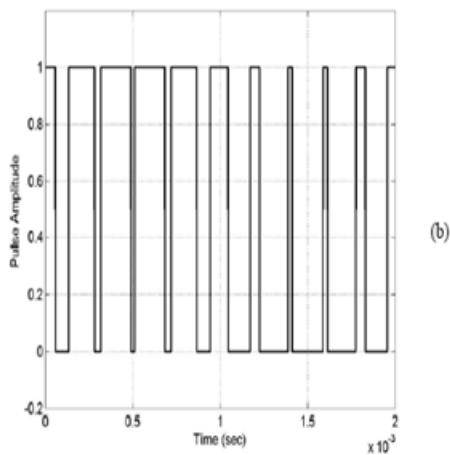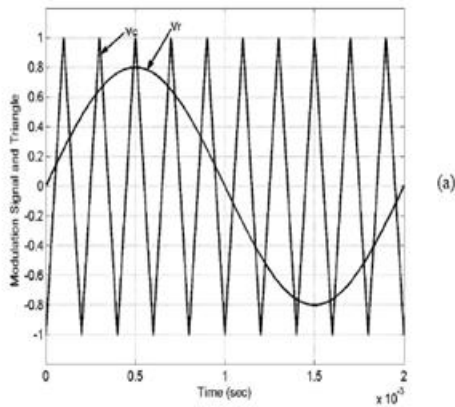
Fig2.6 operating mode (t5-t6)

III. PWM

PWM illustration (a) Sine-Triangle Comparison (b) Switching Pulses after comparison.
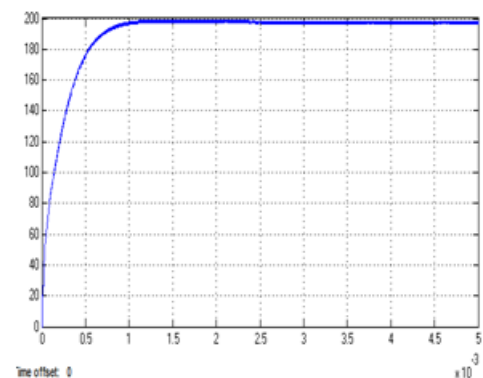
IV. SIMULATION DESIGN:

A simulation design open loop system as shown in **Fig.4.1** is implemented in MATLAB SIMULINK with the help of coupled inductor, voltage clamping circuit and switched capacitor we get desired output voltage level (**Fig.4.2 and Fig4.3**) low voltage output and high voltage waveforms, A modified circuit of the system with single phase inverter is also designed which is shown in **Fig.4.4**. the inverter output is also shown in **fig4.5**.
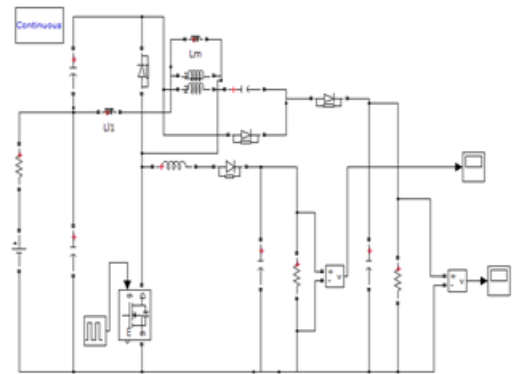
**Fig.4.1. open loop system of SIMO Converter**
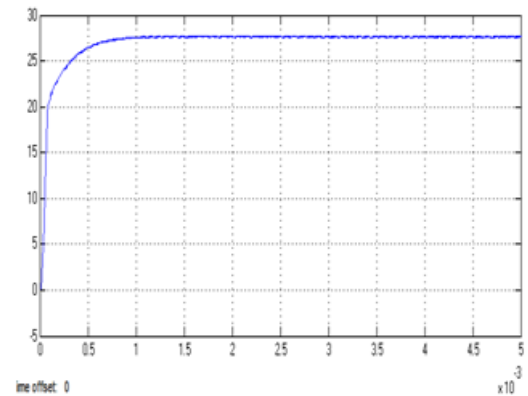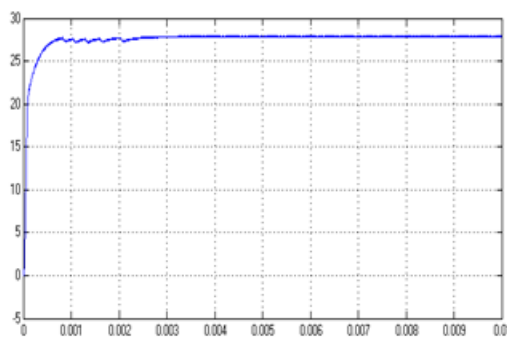

Fig.4.2. Low Voltage Output(28V DC)

Fig.4.3. High voltage output(200V DC)

A simulation design closed loop system as shown in **Fig.4.4** is implemented in MATLAB SIMULINK with the help of coupled inductor, voltage clamping circuit and switched capacitor and PI controllers we get desired output voltage level (**Fig.4.5 to Fig4.6**) low voltage output and high voltage waveforms, A
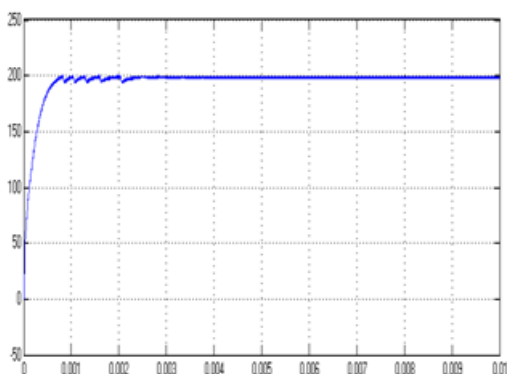
modified circuit of the system with single phase inverter is also designed which is shown in **Fig4.7**. the inverter output is also shown in **fig4.8**.
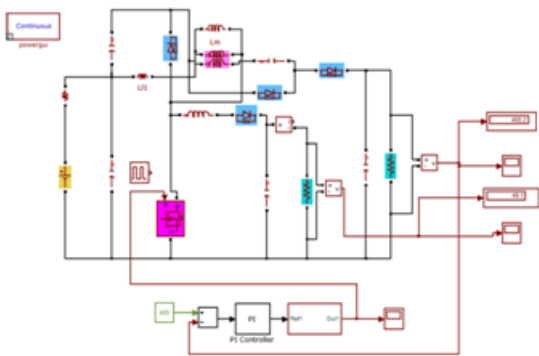
Fig.4.4. closed loop circuit of SIMO Converter with PWM controller

Fig.4.5. low voltage output (28V)

Fig.4.6. high voltage (200V)

V. CONCLUSION:

This project consists of a high-efficiency SIMO dc–dc converter, and this coupled-inductor-based converter was applied well to a single-input power source plus two output terminals composed of an auxiliary battery module and a high-voltage dc bus. For auxiliary railway supply it is better to prefer the above converter which can be used for multiple applications.Open loop and closed loop syslems are developed by using PWM technique. The results are verified using MATLAB software.

REFERENCES:

[1] A. Kirubakaran, S. Jain, and R. K. Nema, "DSP-controlled power electronic interface for fuel-cell-based distributed generation," IEEE Trans. Power Electron., vol. 26, no. 12, pp. 3853–3864, Dec. 2011.

[2] B. Liu, S. Duan, and T. Cai, "Photovoltaic dc-building-module-based BIPV system-concept and design considerations," IEEE Trans. Power Electron., vol. 26, no. 5, pp. 1418–1429, May 2011.

[3] M. Singh and A. Chandra, "Application of adaptive network-based fuzzy interference system for sensorless control of PMSG-based wind turbine with nonlinear-load-compensation capabilities," IEEE Trans. Power Electron. vol. 26, no. 1, pp. 165–175, Jan. 2011.

[4] C. T. Pan,M. C. Cheng, and C.M. Lai, "A novel integrated dc/ac converter with high voltage gain capability for distributed energy resource systems," IEEE Trans. Power Electron., vol. 27, no. 5, pp. 2385–2395, May 2012.

[5] S. D. Gamini Jayasinghe, D. Mahinda Vilathgamuwa, and U. K. Madawala, "Diode-clamped three-level inverter-based battery/ supercapacitor direct integration scheme for renewable energy systems," IEEE Trans. Power Electron., vol. 26, no. 6, pp. 3720–3729, Dec. 2011.

[6] H.Wu, R. Chen, J. Zhang, Y. Xing, H. Hu, and H. Ge, "A family of threeport half-bridge converters for a stand-alone renewable power system," IEEE Trans. Power Electron., vol. 26, no. 9, pp. 2697–2706, Sep. 2012.

[7] M. W. Ellis, M. R. Von Spakovsky, and D. J. Nelson, "Fuel cell systems: Efficient, flexible energy conversion for the 21 st century," Proc. IEEE, vol. 89, no. 12, pp. 1808–1818, Dec. 2001.

[8] T. Kim, O. Vodyakho, and J. Yang, "Fuel cell hybrid electronic scooter," IEEE Ind. Appl. Mag., vol. 17, no. 2, pp. 25–31, Mar./Apr. 2011.

[9] F. Gao, B. Blunier, M. G. Sim˜oes, and A. Miraoui, "PEM fuel cell stack modeling for real-time emulation in hardware-in-the-loop application," IEEE Trans. Energy Convers., vol. 26, no. 1, pp. 184–194, Mar. 2011.

[10] P. Patra, A. Patra, and N. Misra, "A single-inductor multiple-output switcher with simultaneous buck, boost and inverted outputs," IEEE Trans. Power Electron., vol. 27, no. 4, pp. 1936–1951, Apr. 2012

[11] A. Nami, F. Zare, A. Ghosh, and F. Blaabjerg, "Multiple-output DC–DC converters based on diode-clamped converters configuration: Topology and control strategy," IET Power Electron., vol. 3, no. 2, pp. 197–208, 2010.